



Simple Approaches for the Design of Shallow and Deep Foundations for Unsaturated Soils I: Theoretical and Experimental Studies

Mengxi Tan¹ · Xinting Cheng¹ · Sai Vanapalli¹

Received: 13 October 2020 / Accepted: 28 January 2021 / Published online: 18 February 2021
© Indian Geotechnical Society 2021

Abstract Bearing capacity is one of the key properties required in the design of shallow and deep foundations. In conventional engineering practice, simple approaches are widely used for determining the bearing carrying capacity of foundations based on the shear strength parameters of saturated soils. However, foundations are typically placed in part or fully in the soil zone above the natural ground water table, which is in a state of unsaturated condition. The shear strength of unsaturated soils is significantly influenced by the matric suction. The bearing capacity of foundations cannot be reliably determined by extending conventional soil mechanics principles for soils that are in a state of unsaturated condition. This Companion Paper I, introduces how the shear strength can be used as a tool in the interpretation and prediction of the bearing capacity of foundations in unsaturated soils. In addition, both theoretical and experimental studies related to the bearing capacity of unsaturated soils are succinctly summarized. Numerical techniques that can be used for predicting the stress versus settlement behavior used for the design of shallow and deep foundations are summarized in Companion Paper II. The succinctly summarized information in the companion papers are valuable for geotechnical engineers for understanding and implementing the mechanics of unsaturated soils in the design of shallow and deep foundations.

Keywords Matric suction · Unsaturated shear strength · Bearing capacity · Shallow foundations · Pile foundations

Introduction

The behavior of geotechnical infrastructures such as foundations, pavements and retaining structures are significantly influenced by the shear strength of soils. Due to this reason, in conventional engineering practice, simple approaches are widely used for the design of shallow and deep foundations based on the saturated shear strength parameters. In many scenarios, foundations are placed either in part or fully in the vadose zone, which is above the natural groundwater table, where the soil is typically in a state of unsaturated condition. However, the design of foundations is based on conventional saturated soil mechanics principles ignoring the contribution of matric suction of soil in unsaturated conditions. Such an approach contributes to unrealistic estimation of the bearing capacity and the settlement behavior, which are key parameters required in the design of foundations (i.e., both shallow foundations and pile foundations).

Fredlund and Morgenstern [1] proposed a rational framework for interpreting the mechanical behavior of unsaturated soils in terms of two independent stress state variables; namely, net normal stress, $(\sigma_n - u_a)$ and matric suction, $(u_a - u_w)$. In 1978, Fredlund et al. [2] proposed a shear strength relationship extending the Mohr–Coulomb failure criterion for unsaturated soils in terms of two stress state variables. Many experimental studies have been conducted over the last few decades to determine and interpret the shear strength of unsaturated soils (*SSUS*) following this framework [for example, 3–6]. Equation proposed by Fredlund et al. [2] was found to be a valuable tool for explaining the shear strength changes from a saturated condition to unsaturated condition and vice versa. However, experimental studies for determining the *SSUS* need elaborate testing equipment that can be

✉ Sai Vanapalli
Sai.Vanapalli@uottawa.ca

¹ Department of Civil Engineering, University of Ottawa, Ottawa, Canada

performed only with the assistance of trained professionals. In addition, these tests are time-consuming. Due to this reason, several researchers developed empirical and semi-empirical methods for predicting the *SSUS* using the saturated shear strength parameters and the soil–water characteristic curve (*SWCC*) as a tool [for example, 5,7,8]. The *SWCC* is defined as the relationship between the soil water content (volumetric or gravimetric) or degree of saturation and soil suction.

This paper provides a succinct theoretical background information of how *SSUS* information can be used in predicting and interpreting the bearing capacity of shallow and deep foundations. In addition, this framework is supported using model and prototype tests performed in the laboratory and field, respectively. The developed theoretical approaches are consistent with the conventional geotechnical engineering practice applications that are based on saturated soil mechanics. The studies summarized in this paper are encouraging for the geotechnical engineers for implementing the mechanics of unsaturated soils in the design of shallow and deep foundations.

Background

Bishop [9] extended the Terzaghi [10] shear strength equation to describe the effective shear strength of unsaturated soil, which is given below.

$$\tau = c' + [(\sigma_n - u_a) + \chi(u_a - u_w)] \tan \phi' \quad (1)$$

where τ is shear strength of unsaturated soil, c' and ϕ' are the effective shear strength parameters, χ is parameter related to the degree of saturation; terms $(\sigma_n - u_a)$ and $(u_a - u_w)$ are the stress state variables: net normal stress and matric suction.

Fredlund et al. [2] proposed the shear strength equation for unsaturated soil in terms of two independent stress state variables, which is shown as Eq. (2)

$$\tau = c' + (\sigma_n - u_a) \tan \phi' + (u_a - u_w) \tan \phi^b \quad (2)$$

where ϕ^b is the angle of shearing resistance relative to an increase in matric suction. This equation is well established in the literature and provides a rational interpretation of the shear strength behavior of unsaturated soils.

Experimental determination of the *SSUS* however requires expensive equipment, need trained professionals to operate them and is time consuming to perform. For this reason, several researchers [for example, 5,11–14] proposed simple approaches for predicting or estimating the *SSUS*, which typically have form of Eq. (1) or Eq. (2). More comprehensive discussions on the *SSUS* are available in Vanapalli and Fredlund [15] and Vanapalli [16].

The simple approaches proposed by Vanapalli et al. [5] and Fredlund et al. [14] for predicting the *SSUS* are widely used in the literature. In these approaches, shear strength is predicted using the effective shear strength parameters (i.e., c' and ϕ') and the *SWCC* (Eq. 3)

$$\begin{aligned} \tau &= c' + (\sigma_n - u_a) \tan \phi' + (u_a - u_w) (S^\kappa) \tan \phi' \\ \tan \phi^b &= S^\kappa \tan \phi' \end{aligned} \quad (3a)$$

$$\begin{aligned} \tau &= c' + (\sigma_n - u_a) \tan \phi' + (u_a - u_w) \left(\frac{\theta - \theta_r}{\theta_s - \theta_r} \right) \tan \phi' \\ \tan \phi^b &= \left(\frac{\theta - \theta_r}{\theta_s - \theta_r} \right) \tan \phi' \end{aligned} \quad (3b)$$

where θ is the volumetric water content of the soil, θ_s and θ_r are, respectively, the saturated and residual volumetric water contents, S is degree of saturation. The fitting parameter κ varies for different soils and is strongly related to the plasticity index, I_p [15, 17, 18]. In Eqs. (3a) and (3b), $[c' + (\sigma_n - u_a) \tan \phi']$ represents the saturated shear strength. The terms, $[(u_a - u_w) S^\kappa \tan \phi']$ and $[(u_a - u_w) ((\theta - \theta_r)/(\theta_s - \theta_r)) \tan \phi']$, respectively, in Eqs. (3a) and (3b), represent the contribution of the matric suction toward the shear strength.

Figure 1a shows drying *SWCC* for a typical fine-grained soil. Three key stages, namely boundary effect zone (BEZ), transition effect zone (TEZ) and residual zone of saturation (RZS) can be identified in this *SWCC*. All the soil pores are filled with water in the BEZ and the soil is in a state of saturated condition, in spite of soil suction. The value of matric suction at which air enters into the largest pores of soil is referred to as the air-entry value. The soil water content starts to reduce rapidly (i.e., desaturates) with a further increase in the matric suction in the TEZ. The water menisci area which is continuous within the soil particles or aggregates in the BEZ becomes discontinuous during the soil desaturation process in the TEZ as shown in Fig. 1a. The desaturation phase in the TEZ is typically associated with the movement of water in the liquid phase. In the RZS, significantly large suction changes are necessary to achieve even small changes in the water content. The water content reduction in this zone is mostly in the vapor phase as there are no continuous paths for the water to flow in the liquid phase. The water menisci in the RZS is typically small. As a stress state variable, suction contributes to shear strength along the wetted area of contact of soil particles or aggregates. Due to this reason, the shear strength increases linearly in the BEZ (i.e., $\tan \phi^b = \tan \phi'$) when the matric suction is lower than the air entry value shown in Fig. 1b. This is because matric suction is effectively transmitted along the wetted area of contact, which is 100%. However, there will be a nonlinear increase in shear

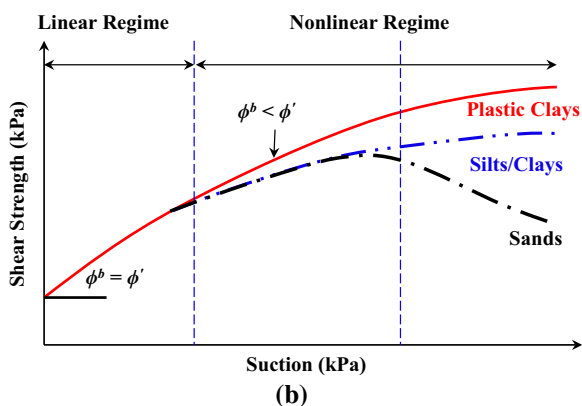
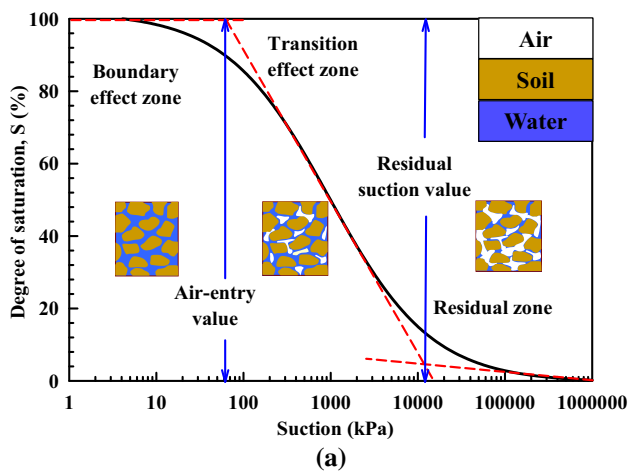


Fig. 1 Relationship between the SWCC and shear strength of unsaturated soils (modified after Vanapalli [16]): **a** typical soil water characteristic curve; **b** shear strength of unsaturated soils in various zones

strength in the TEZ as the suction increases. The matric suction acts along the discontinuous wetted area of contact of soil particles within the TEZ. Therefore, the angle of shearing resistance with respect to suction ϕ^b is less than the angle of shearing resistance ϕ' . The trends in the variation of the bearing capacity of unsaturated soils prior to RZS are consistent with the shear strength behavior [19], which are discussed in greater detail in later sections. In the RZS, for example, sand desaturates at a relatively fast rate and has a low water content (i.e., low degree of saturation). In other words, there is a limited wetted area of contact. Due to this reason, suction in spite of being a higher value compared to BEZ and TEZ, may not be transmitted effectively to all the soil particles at their contact points [5]. Therefore, shear strength in coarse-grained soils typically decreases. Such a behavior can be observed from experimental results by Donald [20]. However, fine-grained soils such as clays may not have a well-defined residual state. Considerable water (in the form of adsorbed water) in clay at residual stage may still be available to transmit suction

effectively. Due to this reason, the shear strength of clays typically increases in the RZS. However, shear strength of certain fine-grained soils such as silts decreases gradually over a large suction range (Escario and Juca [21]). These results suggest that the nonlinear shear strength behavior of unsaturated soils should be considered in the rational design of geotechnical infrastructure. The sections that follow summarize experimental results of bearing capacity of both shallow and deep foundations of unsaturated soils; in addition, bearing capacity is also predicted using SWCC as a tool similar to the SUSS as a tool.

Theoretical Studies

Shallow Foundations

Effective stress approach (ESA) and total stress approach (TSA) are widely used in conventional geotechnical engineering practice for interpreting the bearing capacity of drained and undrained loading conditions, respectively, for saturated soils. Similar approaches can also be used for unsaturated soils and are referred to as modified effective stress approach (MESA) and total stress approach (MTSA).

Modified Effective Stress Approach (MESA)

Terzaghi [10] proposed Eq. (4) for determining the bearing capacity of strip foundations assuming general shear failure condition. Vanapalli and Mohamed [22] extended the Terzaghi [10] equation (Eq. 4) and proposed a bearing capacity equation (Eq. 5a and 5b) for unsaturated soils. Equation (5a) was originally proposed for surface square footing. This equation can be modified as Eq. (5b) taking account of the influence of overburden stress associated with embedded foundation. There is a smooth transition between Eqs. (5a and 5b) and (4) used for unsaturated and saturated soils. In other words, when the matric suction is equal to zero, Eq. (5a and 5b) takes the form as the Terzaghi's equation (i.e., Eq. 4). Equation (5a and 5b) can also be used as a tool to predict the nonlinear variation of the bearing capacity with respect to matric suction using the effective shear strength parameters of saturated soil (i.e., c' and ϕ') and the SWCC. The term $S^p \tan \phi'$ describes the shear strength contribution with respect to matric suction toward the bearing capacity.

$$q_{ult(sat)} = c'N_c + \gamma D_f N_q + 0.5B\gamma N_\gamma \tag{4}$$

$$q_{ult(unsat)} = \left[\begin{aligned} &c' + (u_a - u_w)_b(1 - S^\psi) \tan \phi' \\ &+ (u_a - u_w)_{AVR} S^\psi \tan \phi' \end{aligned} \right] N_c \xi_c + 0.5B\gamma N_\gamma \xi_\gamma \tag{5a}$$

$$q_{ult(unsat)} = \left[\begin{aligned} &c' + (u_a - u_w)_b(1 - S^\psi) \tan \phi' \\ &+ (u_a - u_w)_{AVR} S^\psi \tan \phi' \end{aligned} \right] N_c \xi_c + \gamma D_f N_q \xi_q + 0.5B\gamma N_\gamma \xi_\gamma \tag{5b}$$

where $q_{ult(sat)}$, $q_{ult(unsat)}$ are the ultimate bearing capacity for saturated soil and unsaturated soils, B is the width of footing, γ is soil unit weight, N_c , N_q , N_γ are the bearing capacity factors [10, 23], $(u_a - u_w)_b$ is the air-entry value, ξ_c , ξ_q , ξ_γ are shape factors [24], D_f is the footing embedment depth. $(u_a - u_w)_{AVR}$ is the average matric suction value.

The average matric suction value is defined as the value at the centroid of the suction distribution profile within depth of $1.5B$ or $2B$ (i.e., the predominant stress bulb zone beneath the foundation). Ψ is the fitting parameter that is strongly related to the I_p . Vanapalli and Mohamed [22] proposed an equation (Eq. 6) of Ψ with experiments results of sands, Botkin Pit Silt and glacial till shown in Fig. 2.

$$\psi = -0.0031(I_p)^2 + 0.34(I_p) + 1 \tag{6}$$

Vanapalli and Oh [25, 26] suggested that Ψ can be typically assumed to be 3.5 for fine grained soils with plasticity index, I_p values greater than 8% based on the results of in-situ plate load tests. A value of Ψ equal to 1 is suggested for coarse grained soils with $I_p = 0$. They also summarized that different rates of loading can influence values of Ψ .

Oh and Vanapalli [27] also proposed a methodology using Eq. (5) to evaluate the stress versus settlement relationship. This method was developed by assuming the stress and settlement relationship in the elastic and plastic zones as two straight lines (i.e., linear). The slope of the

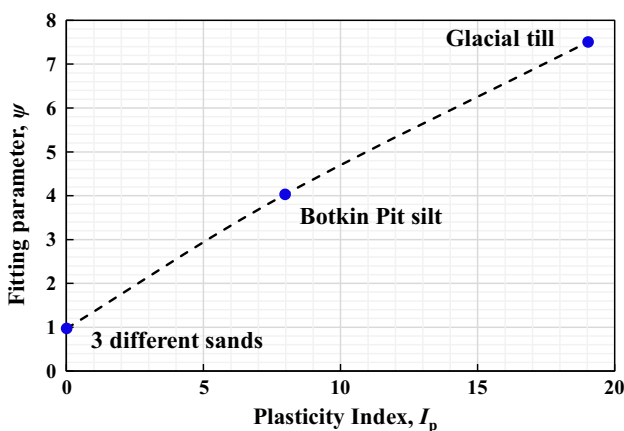


Fig. 2 Relationship between the soil plasticity index and the fitting parameter Ψ

elastic line is equal to the modulus of elasticity of the soil. Oh et al. [28] proposed Eq. (7) for predicting the variation of modulus of elasticity with respect to matric suction.

$$E_{unsat} = E_{sat} \left[1 + \alpha \frac{(u_a - u_w)}{(P_a/101.3)} (S^\beta) \right] \tag{7}$$

where E_{unsat} and E_{sat} are the elastic modulus of unsaturated soil and saturated soil, respectively. P_a is the atmosphere pressure (101.3 kPa). α and β are fitting parameters, $\beta = 1$ for coarse grained soil [28] and $\beta = 2$ [29] for fine grained soil. α value is related to the ratio of footing size to soil particle size and the plasticity index, I_p [28, 29]. The proposed MESA approach has been validated with experimental studies for both coarse- and fine-grained soil with matric suction values lower than the residual suction. More details about the experimental studies and the comparisons between the variation of bearing capacity with matric suction from experimental results and predicted values are discussed in later sections.

Modified Total Stress Approach (MTSA)

Studies by Oh and Vanapalli [30] suggest that MESA may not provide reliable results for large suction values in unsaturated fine-grained (UFG) soils. This may be associated with bearing capacity converging close to residual suction value. For such a scenario, drainage condition of UFG soil may not be well-defined. Investigations suggest that the MTSA provides a reasonable bearing capacity for UFG soils at large suction values. Vanapalli et al. [31] proposed the MTSA to interpret the bearing capacity of foundation in UFG soils under undrained loading condition. The method was based on the equation proposed by Skempton [32] shown as Eq. (8).

$$q_{ult} = c_{u(sat)} \times \xi_c \times N_c \tag{8}$$

where q_{ult} is ultimate bearing capacity of the saturated soil; $c_{u(sat)}$ is the undrained shear strength for saturated soils; N_c is bearing capacity factor related to cohesion under undrained loading condition.

Vanapalli et al. [31] replaced the undrained shear strength in Eq. (8) with that of unsaturated soil $c_{u(unsat)}$. Similar to saturated soil, it is assumed that $c_{u(unsat)}$ is equal to $q_{u(unsat)}/2$ from the unconfined compression (UC) test. Therefore, the ultimate bearing capacity of UFG soil will take the form as shown in Eq. (9)

$$q_{ult(unsat)} = \left[\frac{q_{u(unsat)}}{2} \right] \left[1 + 0.2 \left(\frac{B}{L} \right) \right] N_{cunsat} \tag{9}$$

where N_{cunsat} is the bearing capacity factor under unsaturated condition, it is same with that in saturated condition in this equation. L is the foundation length.

The shear strength of UFG soil is derived from UC test results because of two reasons. The first reason is related to the failure mechanism of the foundations associated with UFG soil under undrained loading condition. Several research studies [30–34] suggest that the failure mechanism of a shallow foundation in UFG soil is closely related to the punching shear failure mode shown as Fig. 3. The bearing capacity of the foundation therefore can be considered as a function of the soil compressive strength below the foundation. The soil condition (pore air drained, pore water undrained) can be realized in UC tests. The second reason is UC test is a quick and conventional test compared to other tests such as the constant water content (CW) tests [30].

Oh and Vanapalli [35] proposed Eq. (10), which facilitates to estimate the variation of the undrained shear strength, $c_{u(\text{unnsat})}$ for UFG soils.

$$c_{u(\text{unnsat})} = c_{u(\text{sat})} \left[1 + \frac{(u_a - u_w)}{(P_a/100)} (S^v) / \mu \right] \tag{10}$$

where v and μ are fitting parameters, $v = 2$ for fine grained soil, μ is related to the plasticity index, I_p , given in Eqs. (11a) and (11b).

$$\mu = 9, 8.0 \leq I_p(\%) \leq 15.5 \tag{11a}$$

$$\mu = 2.1088e^{0.0903(I_p)}, 15.5 < I_p(\%) \leq 60.0 \tag{11b}$$

where e is Euler’s number. The above relationship was derived from six sets of UC test results [15, 31, 36–39]. The results derived by the shear strength equation at suction close to the residual suction value should be carefully interpreted [26]. The proposed approach is valuable;

however, more supporting data from field tests can provide more credence for use in geotechnical design practice.

Pile Foundations

End-Bearing Capacity of Piles Embedded in Unsaturated Sands

Theoretical approaches that have been developed for determining the bearing capacity of shallow foundations can be extended with modifications for estimating the end-bearing capacity of pile foundations. For shallow foundations, Vanapalli and Mohamed [22] proposed an approach for predicting the bearing capacity of surface shallow foundation with respect to matric suction, extending the conventional approach used for saturated soils. In this approach, the effective cohesion, c' term is replaced with total cohesion, c_a for determining the variation of bearing capacity of unsaturated soils taking account the influence of matric suction. The same equation (i.e., Eq. 12) can be also used for predicting the variation of total cohesion, c_a with respect to matric suction. The information of the effective shear strength parameters and the SWCC is required for extending this approach.

$$c_a = c' + (u_a - u_w)_b (1 - S^{\psi_{BC}}) \tan \phi' + (u_a - u_w)_{AVR} S^{\psi_{BC}} \tan \phi' \tag{12}$$

where, Ψ_{BC} = fitting parameter with respect to bearing capacity ($\Psi_{BC} = 1$ for nonplastic soil).

Vanapalli et al. [40] extended this approach to predict the end-bearing capacity $Q_{p(us)}$ of single piles in unsaturated soils. Three conventional methods originally proposed by Terzaghi [10], Hansen [41] and Janbu [42] for estimating the end-bearing capacity of piles in saturated soils were used in extending this approach. The soil above the pile was assumed as an equivalent surcharge, q . Limit equilibrium conditions are used to determine the end-bearing capacity based on failure patterns around the pile tip. The conventional Terzaghi [10] and Hansen [41] / Janbu [42] equations were modified as Eqs. (13) and (14), respectively.

$$Q_{p(us)} = A_p \left([c' + (u_a - u_w)_b (1 - S^{\psi_{BC}}) \tan \phi' + (u_a - u_w)_{AVR} S^{\psi_{BC}} \tan \phi'] N_{cs} + q' N_q + 1/2 B \gamma N_{\gamma s} \right) \tag{13}$$

$$Q_{p(us)} = A_p \left([c' + (u_a - u_w)_b (1 - S^{\psi_{BC}}) \tan \phi' + (u_a - u_w)_{AVR} S^{\psi_{BC}} \tan \phi'] N'_{\gamma} d_c + \eta q' N'_{\gamma} d_q + 1/2 B \gamma N'_{\gamma} \right) \tag{14}$$

where A_p is pile base area, q' is vertical effective stress at the level of pile base, γ is unit weight of soil beneath the

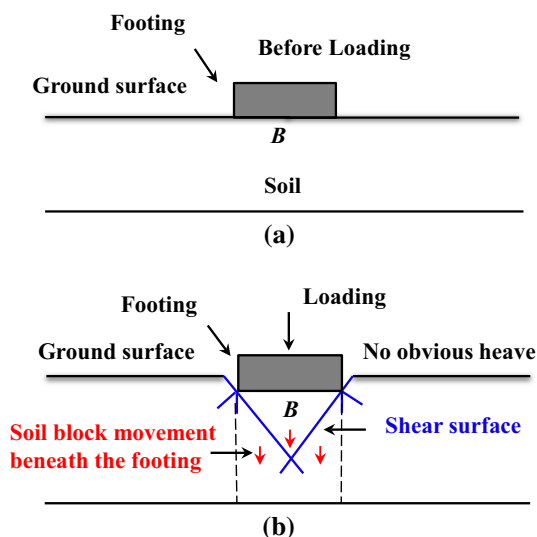


Fig. 3 Schematic of common punching failure mechanism in unsaturated fine-grained (UFG) soils beneath the foundation: a before loading; b during loading

pile, B is pile diameter, s_c, s_γ are shape factors with respect to cohesion and unit weight of soil, respectively ($s_c = 1.3$ and $s_\gamma = 0.6$ for round pile foundation). $N_c, N_q, N_\gamma, N'_c, N'_q, N'_\gamma$ are bearing capacity factors that are functions of soil friction angle, d_c, d_q are depth factors. More details about the information related to the determination of bearing capacity factors are available in Vanapalli et al. [40].

Pile Shaft Carrying Capacity in UFG Soils

Vanapalli and Taylan [43] modified three conventional semi-empirical approaches (i.e., α method proposed by Skempton [44], β method proposed by Burland [45], λ method by Vijayvergiya and Focht [46] for saturated soils) to predict the variation of shaft carrying capacity of pile foundations in UFG soils.

Modified α method The α method was originally proposed by Skempton [44] to determine the shaft resistance of piles placed in saturated cohesive soils extending the total stress approach (TSA) (i.e., $\phi = 0$ concept). In this conventional method, the average shaft friction that develops for carrying the load is related to the mean undrained shear strength by an empirical coefficient α , which is typically less than unity. Extending the same approach, the shaft carrying capacity of pile Q_f under undrained loading conditions in UFG soils can be estimated using Eq. (15).

$$Q_f = f_s \times A_s = \alpha c_u \pi d L$$

$$= \alpha c_{u(\text{sat})} \left[1 + \frac{(u_a - u_w)}{(P_a/101.3)} S^v / \mu \right] \pi d L \quad (15)$$

where d is the pile diameter and L is the length of pile.

Modified β method Burland [45] proposed β method to calculate shaft carrying capacity by extending effective stress approach (ESA). The total stress approach (TSA) is suitable for clayey soils; however, ESA can be used for all soil types. When the displacement between piles and clay is relatively large, the pile shaft friction is mainly influenced by lateral effective stress. Vanapalli and Taylan [43] proposed a modified β method to determine pile shaft resistance in unsaturated soils. The ultimate shaft capacity of a single pile in unsaturated soils $Q_{f(\text{us})}$ consists of the contribution from matric suction $Q_{(u_a - u_w)}$ and conventional shaft resistance Q_f under saturated conditions.

$$Q_{f(\text{us})} = Q_f + Q_{(u_a - u_w)} \quad (16)$$

For fine-grained soils, the apparent cohesion c'_a under drained loading condition is due to the contribution of the shaft carrying capacity. Thus, the ultimate shaft capacity of single pile in unsaturated soils $Q_{f(\text{us})}$ can be written as:

$$Q_{f(\text{us})} = [c'_a + \beta(\sigma'_z) + (u_a - u_w)(S^\kappa)(\tan \delta')] \pi d L \quad (17)$$

where S is the degree of saturation, κ is fitting parameter used for shear strength. The fitting parameter κ can be obtained from the relationships proposed by Vanapalli and Fredlund [15]. σ'_z is the horizontal effective stress acting on the pile and δ' is the effective friction angle of the pile-soil interface, β is Burland–Bjerrum coefficient is equal to $K_0 \tan \delta'$, where K_0 is earth pressure coefficient. For bored piles, the angle δ' is commonly assumed to be equal to the angle of shearing resistance of the surrounding soil, ϕ' , for practical purposes.

Modified λ method Vijayvergiya and Focht [46] suggested λ method to predict pile shaft carrying capacity, which combines TSA and ESA. This method assumes that the unit skin friction has a relationship with both vertical effective stress and the undrained shear strength. The shaft resistance per unit area $f_{s(\text{avg})}$ can be estimated by the following equation:

$$f_{s(\text{avg})} = \lambda (\sigma'_{v(\text{avg})} + 2c_u) \quad (18)$$

where $\sigma'_{v(\text{avg})}$ is the mean effective stress along the pile shaft, λ is frictional capacity coefficient which is a function of entire embedded depth of pile. The λ method was modified by Vanapalli and Taylan [43] to estimate the shaft carrying capacity of single pile $Q_{f(\text{us})}$ with respect to matric suction.

$$Q_{f(\text{us})} = \lambda \left[\sigma'_{v(\text{avg})} + 2c_{u(\text{sat})} \left(1 + \frac{(u_a - u_w)}{P_a/101.3} S^v / \mu \right) \right] \pi d L \quad (19)$$

Also, when matric suction ($u_a - u_w$) equals to zero, Eq. (19) is the same as Eq. (18) for saturated soil conditions.

All the modified approaches (i.e., α method, β method, and λ method) provide a smooth transition of pile shaft carrying capacity from unsaturated to saturated soil conditions. In other words, these equations (i.e., Eqs. 15, 17, 19) take the form of conventional equations used for saturated soils, when matric suction equals a value of zero.

Experimental Studies

Laboratory Tests on Shallow Foundation

Table 1 provides a summary of the experimental studies information along with the proposed equations for interpreting the bearing capacity and settlement of shallow foundations. Laboratory tests on model shallow foundations using the MESA and MTSA methods are introduced in this section. In addition, in-situ tests such as the standard

Table 1 Summary of the experimental studies related to the bearing capacity of shallow foundations in unsaturated soils

Experiments and equation validation				
Bearing capacity and settlement	Modified total stress approach (MTSA) Suitable for fine grain soil	Indian Head till	Unconfined compression (UC) test Model footing test	Vanapalli et al. [31]
		Lateritic soil deposit	Validation: in-situ plate load test (PLT)	Vanapalli and Oh [25]
	Residual cohesive soil		Costa et al. [47]	
		Validation: PLT Consoli et al. [48]	Oh and Vanapalli [30]	
	Modified effective stress approach (MESA) Suitable for coarse and fine grained soils	Unimin (7030) sand	Model footing test	Mohamed and Vanapalli [49, 50]
		Huston sand	Model footing test for plain strain condition	Vanapalli and Mohamed [22, 51]
			Indian Head till	Model footing test
	In-situ tests	Dark-gray silty sand underneath the septic sand	PLT	Oh and Vanapalli [30]
			Standard penetration test (SPT), CPT In-situ foot loading test validation [53]	Mohamed and Vanapalli [54]
	–	Poorly graded fine sand (according to USCS)	PLT (modified UOBCE), Cone penetration test (CPT)	Vanapalli and Mohamed [51]

penetration test (SPT) and plate load test (PLT) are also summarized with the site details and their results. Finally, comparisons between the predicted results from the proposed approach and the measured data from experiments are summarized.

Laboratory Tests on Coarse-Grained Soil

Mohamed and Vanapalli [49], Vanapalli and Mohamed [51] conducted model footing tests in coarse grained sand with the Ottawa Bearing Capacity Equipment (UOBCE, shown in Fig. 4) and the modified UOBCE. The features of the modified UOBCE are similar to UOBCE; however, its test box size and its loading capacity is twice to that of UOBCE. The UOBCE is designed to perform the bearing capacity of both model footing tests in both saturated and unsaturated soils. The UOBCE constitutes of an aluminum tank with dimensions of 900 mm × 900 mm × 750 mm. The front face of the tank is constructed with a transparent acrylic plate. This transparent plate is helpful for the examination of the thickness of the soil layer during installation and for the observation of water table changes. Stiffeners (Fig. 4, Item 14) were set along the tank side to prevent lateral bending or bulging. First, 50 mm layer of clean aggregate (Fig. 4, Item 16) was placed at the bottom of the test tank with a thin geotextile sheet (Fig. 4, Item 7)

on the top. The geotextile sheet is a porous barrier between the soil and the aggregate. Gradual free movement of water is assured through the bottom aggregate and geotextile sheet layer. The sand was then allowed to fall freely from a 1 m height with a V-shaped hopper (Fig. 4, Item 3) to achieve the maximum relative density. The hopper which is able to hold 25 kg soil can be monitored to move horizontally and vertically using a side motor with horizontal chain and the side crank with cables on four rollers on the top of the frame (Fig. 4, Item 1). The soil was further compacted using a 5 kg compactor after achieving a uniform relative density of 55% by allowing the soil spread with the V-shaped hopper. An average relative density value of 64% was achieved after compaction of soil; which was verified by collecting soil samples at various depths in the tank with an aluminum cups. The sand was then saturated by raising the water level from the bottom of the tank using the water supply valve in Fig. 4 (Valve A). The water supply pipe has a diameter of 20 mm which branches into 4 small pipes with a diameter of 12.5 mm to assure the saturation process is gradual and uniform from the base to the surface of the soil. The water level in the tank can be adjusted by inspecting the piezometers (Fig. 4, Item 5). The water supply valve was closed when the water level reached the soil surface. After saturation, the water could be controlled with the drainage valve in Fig. 4 (Valve B) to

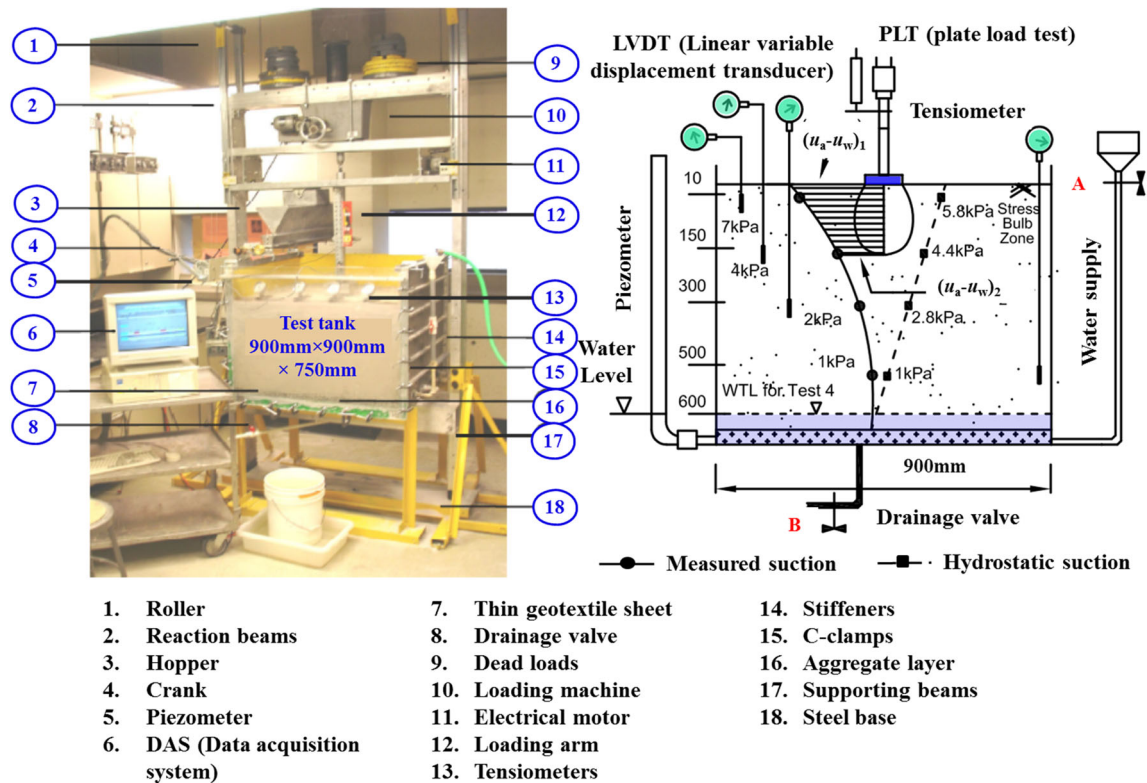


Fig. 4 University of Ottawa Bearing Capacity Equipment (UOBCE) (modified after Vanapalli and Mohamed [51])

reach the target water level and the corresponding target matric suction. The target matric suction was the average matric suction in the stress bulb beneath the foundation (i.e., 2, 4 and 6 kPa). The matric suction was measured using four tensiometers placed at different depth levels in the tank.

The model footing test was conducted after achieving equilibrium conditions with respect to target matric suction value. Mohamed and Vanapalli [49] conducted model footing test with two square model footings with sizes of 100 mm × 100 mm and 150 mm × 150 mm. The distance between the model footing edge and the tank sides was four times of the footing width to alleviate boundary effects. Linearly Variable Displacement Transducer (LVDT) was used to measure the displacement of the footing and was connected to the data acquisition system (DAS, Fig. 4, Item 6). The LVDT tip was placed directly on the surface of the model footing. A load cell which was also connected to the DAS was mounted on the loading arm. The bearing capacity of the footing was measured by loading the footing with a rate of 1.2 mm/min.

Figure 5 provides comparisons between the measured bearing capacity and the predicted results using Eq. (5a). The effective shear strength parameters required for bearing capacity estimation using Eq. (5a) are derived from direct shear tests. The average matric suction method has

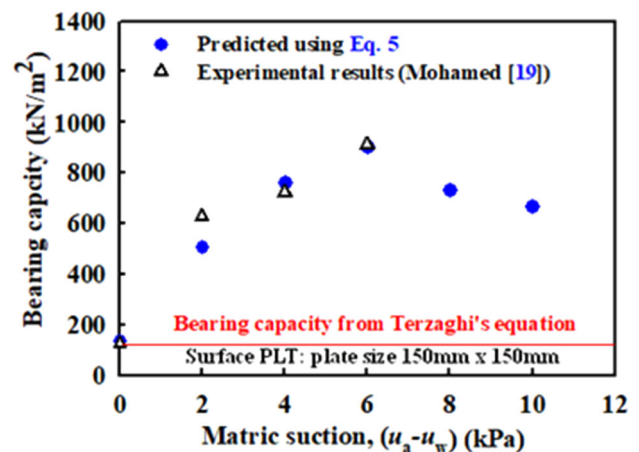


Fig. 5 Comparison between the measured bearing capacity and predicted bearing capacity of sand using Eq. (5)

been used in estimation of the bearing capacity. The value of average matric suction is the centroid of the matric suction distribution profile in the stress bulb zone (shown in Fig. 4), which was discussed earlier. The degree of saturation corresponding to the average matric suction used for Eq. (5a) was derived from the SWCC of the soil. Good agreement has been found in Fig. 5 between the experimental results and the predicted values. The bearing capacity of footing was found increase until reaching the

average matric suction value of 6 kPa, which is approximately, the residual suction value. It is important to note that the measured data were restricted to matric suction range 0–6 kPa because of the limitations with respect to the depth of test box. The reductions in predicted bearing capacity values for matric suction values greater than 6 kPa can be explained with the discontinuous water phase shown in Fig. 1. For such a scenario, sand desaturates and the discontinuous water phase in soil leads to changes in both stress state and soil–air–water particle contact area, which is typically limited. As a result, suction may not be transmitted effectively to all the soil particles which leads to reduction both in the shear strength and bearing capacity, extending the arguments discussed earlier with Fig. 1b.

Cone penetration test (CPT) results are also widely used in conventional engineering practice for estimating bearing capacity of soils. Besides model footing tests, Mohamed et al. [55] conducted CPT within the UOBCE discussed earlier to investigate the bearing capacity of sand taking account of the influence of matric suction. The test equipment for the CPT is shown in Fig. 6. The test cone was fabricated with harden steel with a tip angle of 60°. A diameter of 40 mm was chosen following the recommendations by ASTM D 5778 [56]. Two horizontal aluminum channel sections and a shaft (Fig. 6, Item 6) were set to prevent deformation of the loading rod to achieve vertical penetration of the cone. The water table in the tank was controlled with the water supply valve and drainage valve (Fig. 4, Valve A, Valve B). Tensiometers (Fig. 6, Item 2) are placed at different depths above the water table for the matric suction measurement. Similar to the model footing

test, the cone resistance q_c was determined using a strain rate of 1.2 mm/min in four different suction profiles (i.e., average matric suction: 0, 1, 2, 6 kPa).

Mohamed et al. [55] proposed two equations (Eqs. 20a and 20b) for estimating the bearing capacity of foundations using CPT results by correlating them with the model footing test results

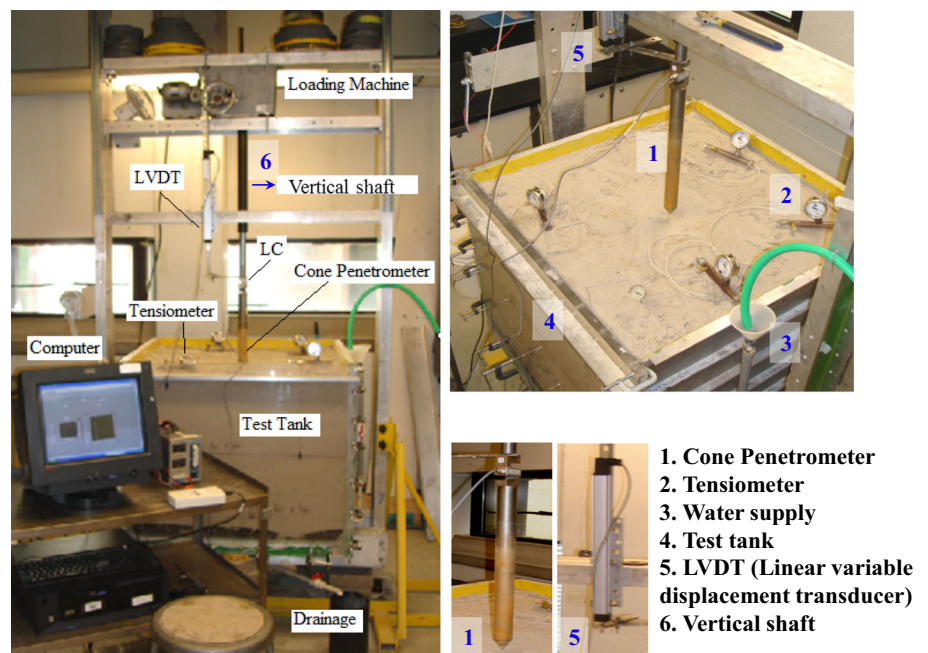
$$q_{\text{usat}} = \Theta (q_{\text{csat}}), \Theta = 0.15/B^{0.63} \tag{20a}$$

$$q_{\text{u(unsat)}} = \Omega (q_{\text{c(unsat)}}), \Omega = 0.19/B^{0.68} \tag{20b}$$

where q_{usat} and $q_{\text{u(unsat)}}$ are bearing capacity for saturated sand and unsaturated sand, Θ and Ω are correlation factors related to the footing width B , q_{csat} and $q_{\text{c(unsat)}}$ are the average cone resistance in saturated and unsaturated soil. The average cone resistance is similar to the average matric suction method discussed earlier in the paper; the influence zone for the average calculation is set as $1.5B$ from the footing base level.

Results summarized in Fig. 7 suggest a good agreement between the measured bearing capacity from the model PLTs (i.e., model footing), in-situ footing load tests (FLT) [53, 57] and that estimated with Eq. (20). The coefficient of determination R^2 is equal to 0.95. Equation (20) provides a reasonable estimation of the bearing capacity from the CPT results. However, more studies are required with various sizes of footings and soils in the field such that they can be used by geotechnical engineers for practice applications with greater degree of confidence.

Fig. 6 CPT equipment for determining the bearing capacity of unsaturated soils (modified after Mohamed [19])



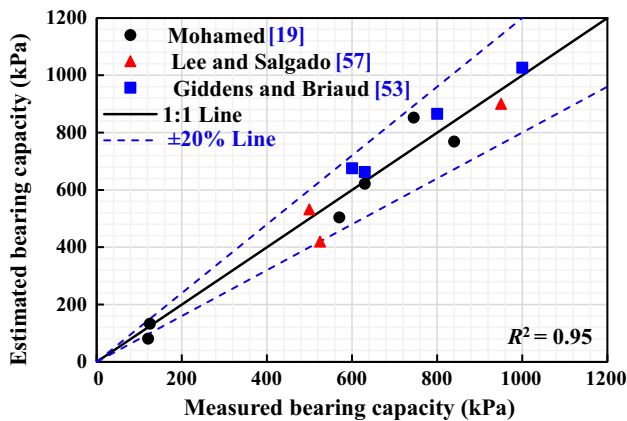
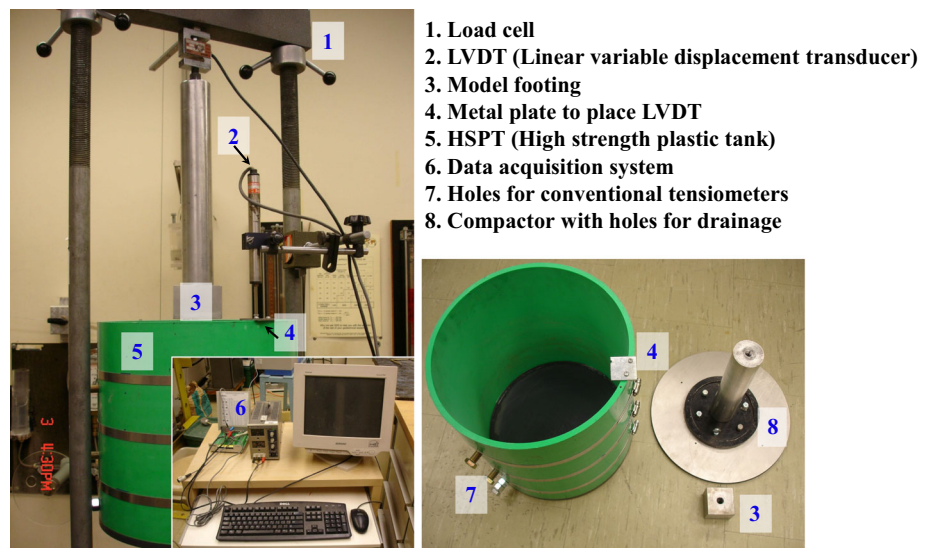


Fig. 7 Comparison between the measured data from laboratory surface PLTs, in-situ footing load test (FLT) and estimated bearing capacity using Eq. (20)

Laboratory Tests on Fine-Grained Soil

Vanapalli et al. [31] performed a series of model footing tests on a glacial till from Indian Head under undrained loading conditions. Figure 8 provides details of the experiment setup. The glacial till was compacted in a high strength plastic tank (HSPT) (Fig. 8, Item 5) with dimensions of 300 mm × 300 mm × 12.7 mm (Diameter × Height × Thickness) to perform model footing tests with 50 mm × 50 mm footing dimensions. The ratio of the diameter of the HSPT to the footing width was set as six based on the published studies to alleviate the influence of boundary conditions [58–61]. Three clamps were placed around the HSPT to alleviate strain during the test. A metal plate (Fig. 8, Item 4) was positioned at the top of the tank to place LVDT to measure the displacement of the footing. The soil was prepared with an initial water content of 13.2% and was compacted to a dry density of 14.4 kN/m³

Fig. 8 Equipment for used for determining the bearing capacity of model footing in unsaturated fine-grained (UFG) soil (modified after Oh and Vanapalli [30])



using static compaction stress of 350 kPa. The soil was statically compacted in five layers with the specially designed compactor (Fig. 8, Item 8). Four holes were drilled on the circular compactor for drainage. The compaction of soil layers stopped until no further displacement was observed. Prior to placing a new layer of soil, the surface of previous layer was scarified. After completing the compaction of all five layers, the soil was saturated by allowing water entering the soil through the drainage holes in the compactor (Fig. 8, Item 8). At the same time, the special compactor was fixed on the surface of the soil to prevent soil swelling. The HSPT was then submerged into the water for 3 days to ensure the soil was fully saturated. After removing the HSPT from water, four tensiometers were installed at different depth levels in the tank (10, 40, 80, 120 mm) (Fig. 8, Item 7). The soil was then subjected to air drying for several days to achieve the target matric suction profile which were monitored using the tensiometers. Due to the air drying, the top soil layer would have a rather high matric suction. The HSPT was wrapped tightly and put in a humidity controlled box for more than 14 days to achieve equilibrium conditions with respect to matric suction profile. The model footing test was conducted after taking the HSPT out from the box. Five suction profiles had been considered in the experiments (with average suctions in stress bulb of 0, 55, 100, 160, 205 kPa). The bearing capacity of model footing under each suction profile was determined by applying a rate of loading equal to 1.14 mm/min.

Figure 9 shows good agreement with $R^2 = 0.93$ between the estimated bearing capacity from Eq. (9) and measured bearing capacity from the model footing test. The shear strength used in Eq. (9) is derived from UC test. The soil specimens prepared for UC test were extracted from the

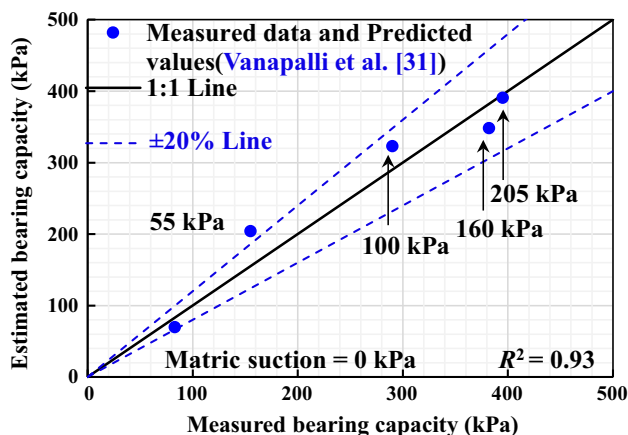


Fig. 9 Comparison between the measured and predicted bearing capacity of square model footing with width of 50 mm

compacted soil outside of the stress bulb below the foundation in the tank. The soil sample may therefore have a similar suction distribution with that in model footing test. Unlike coarse-grained soil, the bearing capacity of footing on fine-grained soil increases with an increase in matric suction for the current study range. This can be explained with Fig. 1b which highlights the shear strength or the bearing capacity of fine grained soil will increase after the air entry value and keep increasing or stay constant beyond the residual suction value.

In-situ Tests on Shallow Foundations

In conventional engineering practice, the in situ bearing capacity of soils is typically determined from PLT, CPT or SPTs [54]. Mohamed and Vanapalli [54] conducted in-situ tests to determine the bearing capacity of sand taking account of the influence of matric suction. The tests were conducted at Carp region in Ottawa, Ontario, Canada. The test site and SPTs, PLTs and tensiometers location are shown in Fig. 10. The site has a sloping terrain with a difference of 2.4 m between the upper and lower levels. Dark-gray silty sand was found underneath the 4.7 m depth of gray sandy soil (known as septic sand) from the upper level surface.

SPT-01 results in Fig. 10b represent saturated condition since it was close to natural ground water table (GWT). The other three SPTs were conducted that represent unsaturated conditions in the upper level region. Each of the three tests had a distance about 12 m between them as shown in Fig. 10a. The SPTs were conducted with a truck mounted equipment following the ASTM D1586 [62] up to depth of 3.5 m from the natural soil surface. The SPT energy efficiency was equal to 60%. More details about the SPT and blow counts are discussed in Mohamed and Vanapalli [54]. A steel plate of 0.2 m × 0.2 m had been

used in the PLTs. Two PLTs were conducted at lower level in different zones of varying matric suction values. PLT-01 was conducted in a saturated condition with zero matric suction recorded on tensiometer. PLT-02 was carried out on a soil suction of 2 kPa. PLT-03 was conducted at upper level with a uniform suction of 8 kPa. All of the three tests were conducted at a depth of 0.15 m. The tensiometers measured the matric suction at the mid-height depth of the stress bulb zone.

Results of the in-situ SPTs showed that the blow count *N* under unsaturated soil condition was much higher than that of saturated soil. The in-situ PLTs also showed that the bearing capacity of the plate on soil with a suction value of 8 kPa was about three times higher than that on saturated soil [54]. Correlations of the SPTs results and PLTs results have been proposed by Mohamed and Vanapalli [54] as Eqs. (21a) and (21b). The equations are based on the CPT and PLT correlation equations proposed by Mohamed et al. [55] that were discussed earlier.

$$q_{all(sat)} = \frac{0.15}{B^{0.63}} \left[0.37 (N_{(sat)})^{0.73} \right] \times 1000 \quad (21a)$$

$$q_{all(unsat)} = \frac{0.19}{B^{0.68}} \left[0.45 (N_{(unsat)})^{0.83} \right] \times 1000 \quad (21b)$$

where $q_{all(sat)}$ and $q_{all(unsat)}$ are allowable bearing capacity for footings on saturated sand and unsaturated sand. The allowable bearing capacity was determined at a settlement of 6 mm of PLT. $N_{(sat)}$ and $N_{(unsat)}$ are the average corrected SPT blow count value in the influence zone (i.e., stress bulb zone within depth of 1.5*B* beneath the footing). Comparisons between the bearing capacity predicted with Eqs. (21a), (21b) and that from different published in-situ test [53, 63] are shown in Fig. 11. Results show a good agreement between the predicted and measured values for various plate sizes. The measured and estimated values of bearing capacity are within the ± 20% deviation line. The proposed equation is promising for use in geotechnical engineering practice.

Laboratory Tests on Deep Foundation

Laboratory Tests on Coarse-Grained Soil

Vanapalli et al. [40] carried out experimental studies to investigate the load versus displacement behavior of single piles in an unsaturated coarse-grained soil (i.e., Unimin Sand). The details of test program are presented in Fig. 12. The soil container was 300 mm in diameter, 700 mm in height and 8 mm in thickness. The model pile used in the tests was stainless steel piles with three different diameters (i.e., 38.30, 31.75, and 19.25 mm) with a length of 350 mm. Three tensiometers were installed at different depths (i.e., 50, 200, 250 mm) from soil surface to measure

Fig. 10 Test site details (modified after Mohamed and Vanapalli [54]): **a** test terrain and SPT, PLT and tensiometer locations; **b** side view of the test site and location

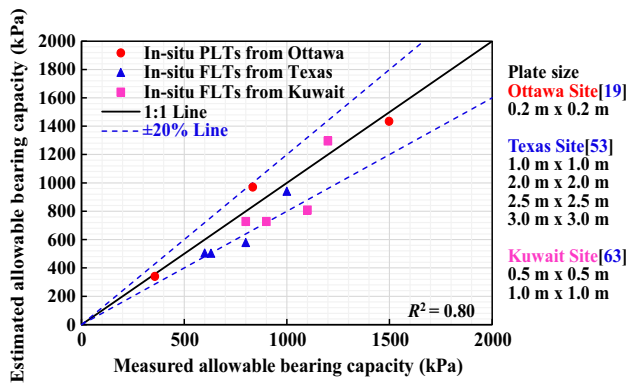
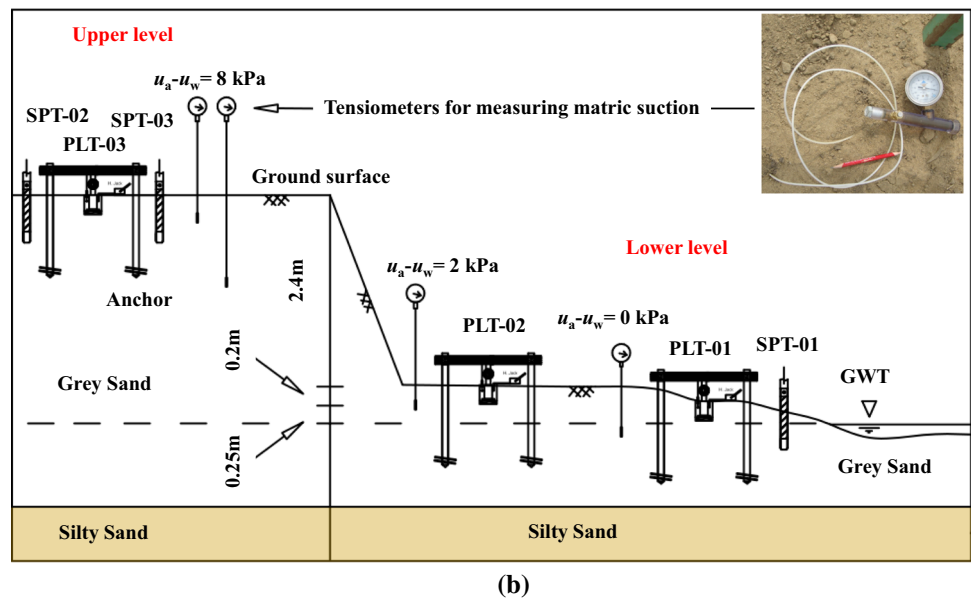
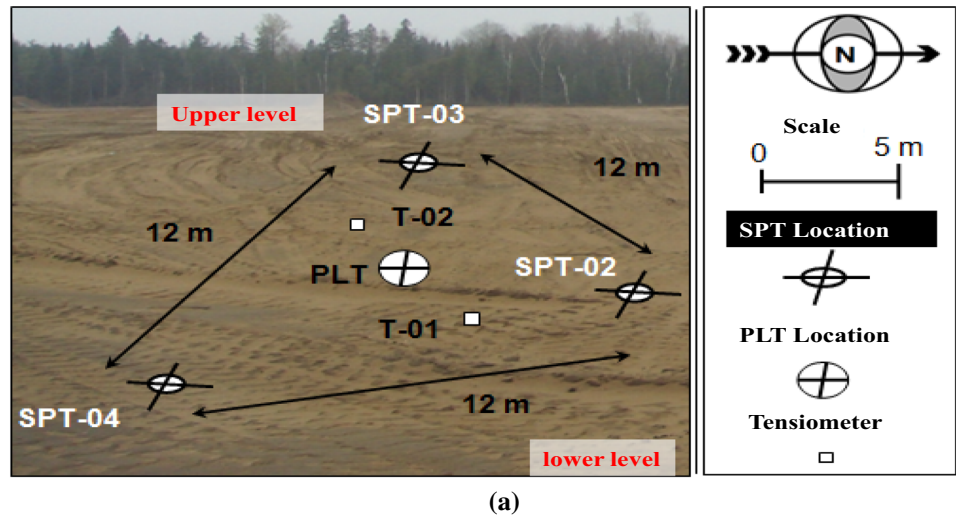


Fig. 11 Comparison between the measured allowable bearing capacity from various test sites and that from estimation using Eq. (21)

and monitor the matric suction values. The water container was connected to water supply/drainage valve at the base of soil container to obtain required water levels using a pulley system. The end-bearing capacity and shaft-bearing capacity of model piles were measured separately. The pile was placed through a hollow sleeve in order to eliminate the contribution of pile shaft resistance toward the total bearing capacity for measuring the end-bearing capacity of the model pile. The cylindrical tube was covered with a thin flexible plastic sheet film on the top of soil sample for measuring the shaft-bearing capacity of the model pile. The plastic film facilitates to prevent the connection between the pile base and soil surface in order to reliably measure of pile shaft bearing capacity. Two different matric suction distribution profiles were achieved by setting one water level at 450 mm deep and the other at 650 mm deep from soil surface in the compacted sand (Fig. 12). The water

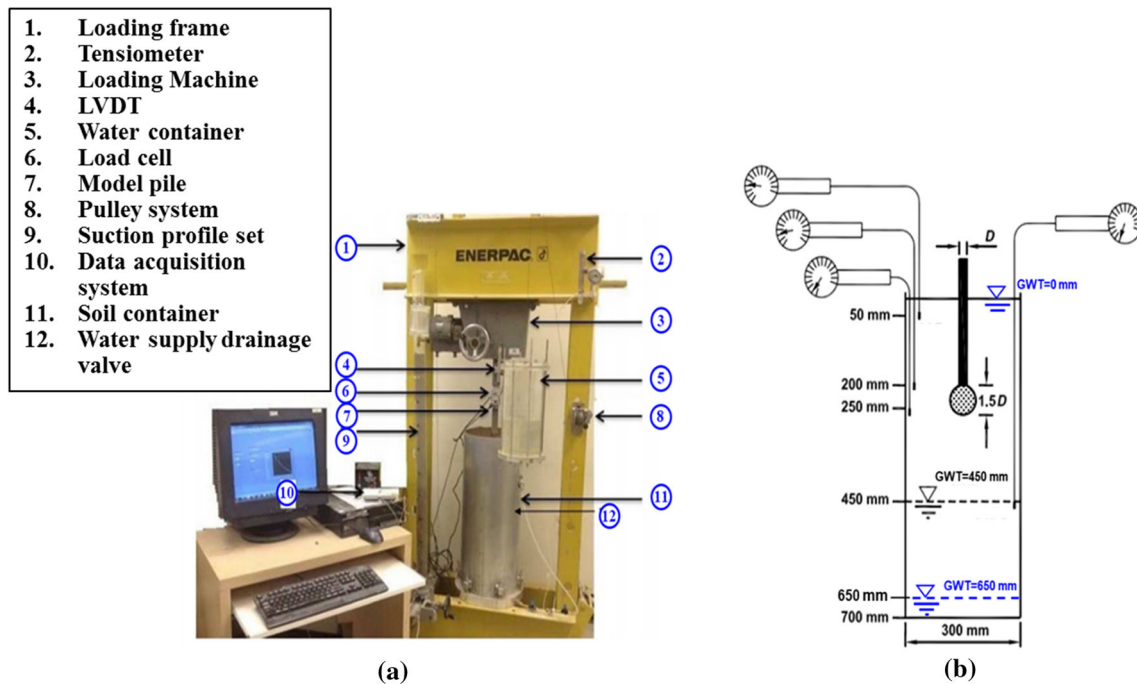


Fig. 12 Details of test program: **a** details of the test setup for determining the load carrying for model pile **b** Cross-sectional schematic of testing program with the water level at 450 and 650 mm from the soil surface (modified after Vanapalli et al. [40])

level was raised from the bottom of the sand to slightly above soil surface to achieve saturated soil conditions. The elevation of water level was adjusted using a pulley system through a thin plastic tube connected to the water container. After an equilibrium time period of 24–48 h, the fully saturated soil condition was ensured. For the purpose of convenience, the average matric suction values of 2 kPa, 4 kPa were used in this study which were achieved maintaining water levels at 450 mm and 650 mm deep from the soil surface, respectively. After achieving equilibrium conditions with respect to targeted matric suction values, the load was applied to the top of the model pile at a rate of 0.7 mm/min to ensure a drained loading condition.

The experiment results showed that the end-bearing capacity of single piles in unsaturated sands was between 2 and 2.5 times higher than that in saturated sands. These results motivated to propose theoretical approaches [22], which were discussed earlier (i.e., Eqs. 13 and 14), for estimating pile carrying capacity taking account of the influence of matric suction in unsaturated soils. Figure 13 shows a good agreement with less than 10% deviation between the measured end-bearing capacity values and those calculated by the modified methods. Relatively high R square values for all cases are also shown in this study. Among three methods, the modified Terzaghi [10] method provides results that are closer to the measured values compared to the other two modified methods.

Al Khazaali and Vanapalli [64] conducted experimental studies to investigate the behavior of single model piles and

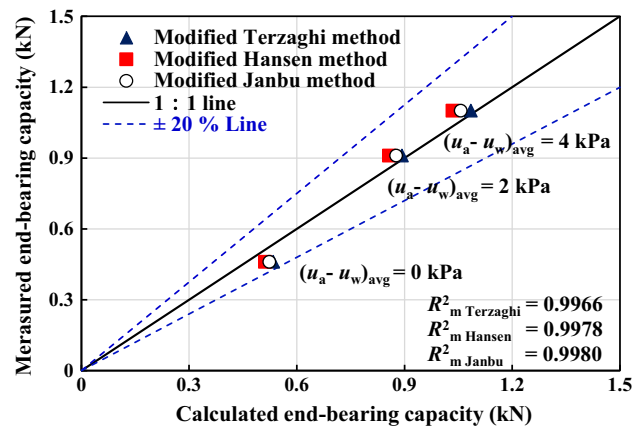
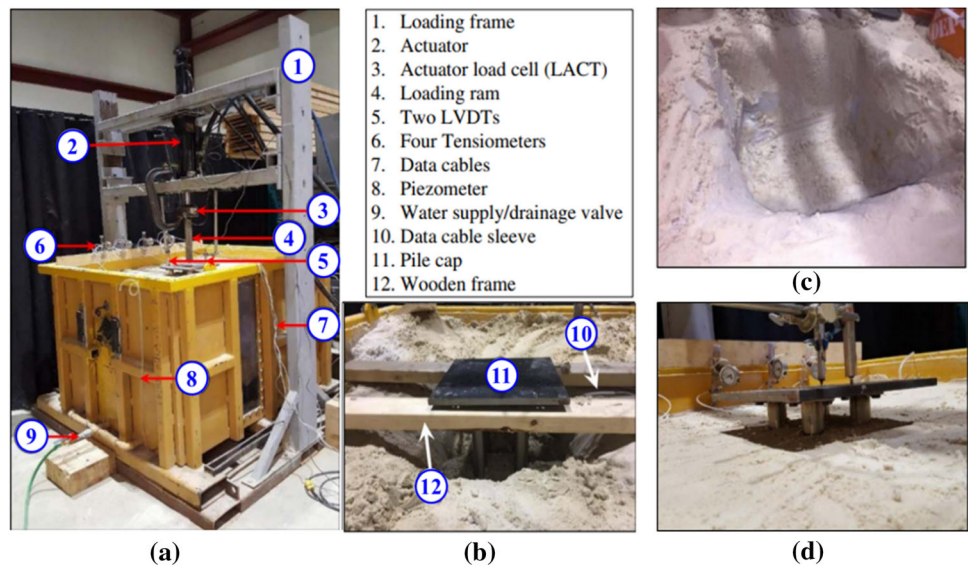


Fig. 13 Comparison between measured end-bearing capacity values and those estimated using the three different modified end-bearing capacity equations (Eqs. 13 and 14) ($D = 38.3$ mm)

2×2 pile groups in saturated and unsaturated sands in the modified UOBCE equipment, which was succinctly discussed earlier. Model piles of 38.1 mm diameter and 300 mm embedded length with smooth and rough shafts with three different pile center-to-center spacing (i.e., $3D$, $4D$, and $5D$) for the pile group, were used in the tests, to investigate the influence of matric suction, roughness of soil-shaft interface, dilation and group effects. A total of 40 tests were performed by varying the water table levels (i.e., 0, 300, 400, 550, and 850 mm deep from the sand surface) to achieve different matric suction profiles. The test setup

Fig. 14 Test setup for model pile group test (modified after Al Khazaali and Vanapalli [64])



and preparation for pile groups performed in modified UOBCE are shown in Fig. 14. First, a square pit was dug in the middle of soil container in Fig. 14c. Then, the model pile or pile group was placed in this pit. The sand surrounding the pile was manually compacted to optimum moisture content while model piles or pile group was supported by wooden frame in Fig. 14b. The water supply/drainage valve connected to the soil container was used to control the saturation and desaturation procedures in the

sand. The load of 0.5 mm/s rate was applied at the top of model pile or pile groups to simulate a drained loading condition.

The results of tests showed that the bearing capacity of both single piles and pile groups were significantly improved due to the contribution of matric suction to shear strength and stiffness of unsaturated soils. The ultimate bearing capacity P_{ult} was observed to increase linearly in the BEZ until suction reached AEV. Then P_{ult} increases

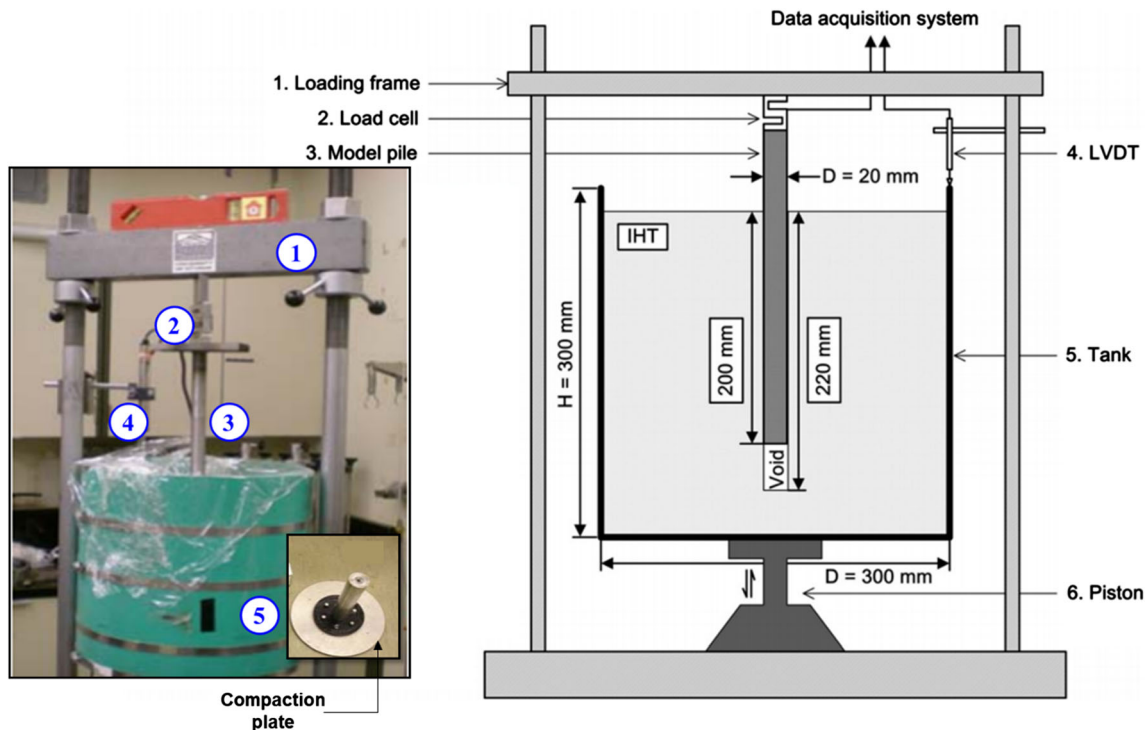


Fig. 15 Test setup for single model pile loading test (modified after Han and Vanapalli [68])

nonlinearly in the TEZ and reduced in the RZS. Based on the tests on model piles fabricated with smooth and rough surfaces, the results indicated that the shaft roughness has significant effect on pile shaft resistance since threaded shaft have more notable influence on behavior of a single pile in comparison with smooth shafts. The results also showed that the stress bulb zone generated by pile groups is several times deeper than it generated by individual piles. The stress state in the unsaturated bulb zone changes due to group action effects, which contribute to variation of moisture regime. Such changes will influence both shear strength and stiffness of soil which in turn influence the bearing capacity of pile groups in unsaturated soils. More comprehensive information is summarized in Al Khazaali and Vanapalli [64].

Laboratory Tests on Fine-Grained Soil

Vanapalli and Taylan [43] have conducted a series of single model pile tests to study the contribution of matric suction on the pile carrying shaft capacity in UFG soils under undrained and drained loading conditions. A glacial till, IHT was used for performing model pile tests. The schematic of the model pile test is shown in Fig. 15. The soil was placed in a 300 mm depth and 300 mm diameter cylinder tank. It was compacted statically under 350 kPa stress using a specially designed compaction plate. The soil samples were compacted at four different initial water contents: (i) $w = 13\%$ (i.e., as-compacted condition, referred as ASCOMP-13%), (ii) $w = 16\%$ (ASCOMP-16%), (iii) $w = 18\%$ (ASCOMP-18%), and (iv) $w = 13\%$ in fully saturated condition (SAT-13%). The SAT-13% condition was achieved by allowing the water to flow downward into the ASCOMP-13% soil sample through the apertures of compaction plate. Axis-translation technique with a modified null pressure plate [65] was used to measure matric suction of soil samples.

After the soil was compacted, a thin wall sampling tube of 18.7 mm was used to drill a vertical hole down to 220 mm deep from the soil surface. Model piles used in this test were stainless steel piles with 20 mm diameter, which was slightly larger than the diameter of sampling tube in order to obtain a good contact between model piles and surrounding soils. The model pile was loaded using a triaxial test loading frame. LVDT was used for measuring the pile displacement and load cell was for measuring the applied load at the top of pile. Model piles were installed to a depth of 200 mm after the borehole drilling was done. A 20 mm depth gap under the base of pile was set up to eliminate the end bearing resistance while loading the model pile. After the preparation of tests, model piles were subjected to a strain rate of 0.0120 mm/min loading to simulate drained loading conditions. This loading rate is

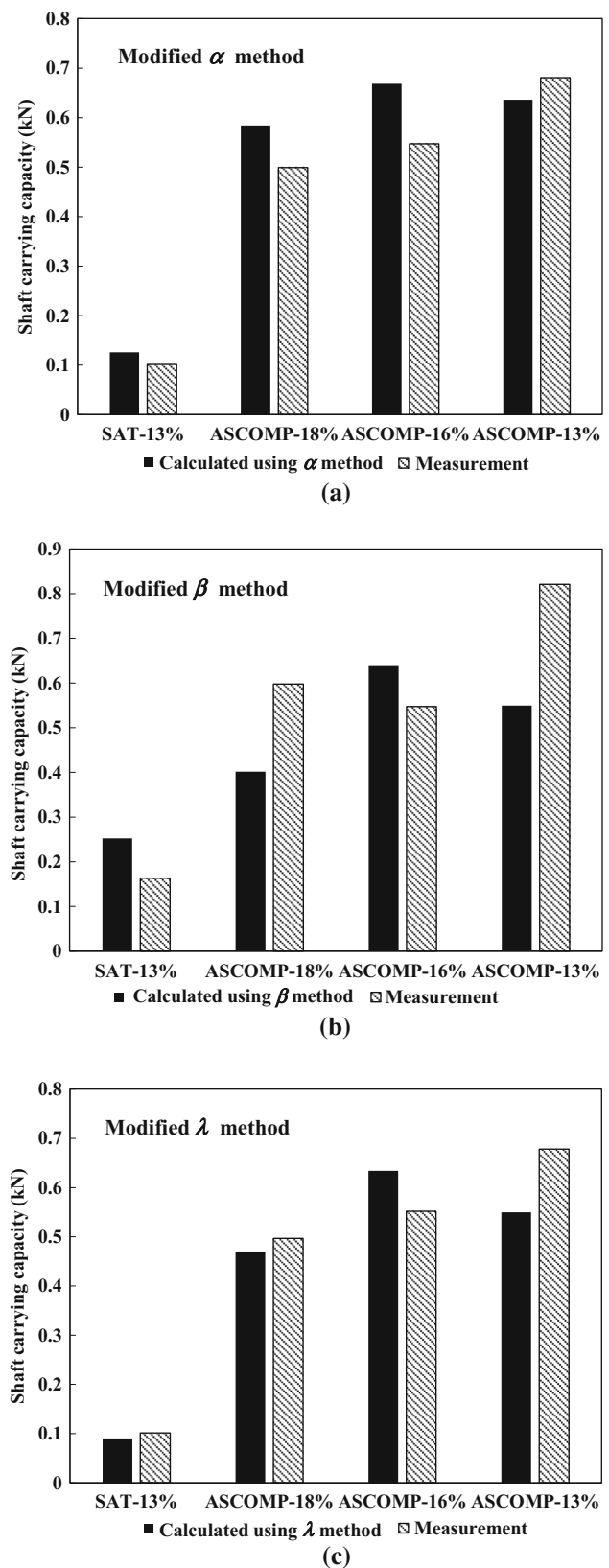


Fig. 16 Comparison between measured and predicted shaft carrying capacity the modified α , β and λ methods

Table 2 Comparison between the measured and estimated undrained shear strength

Sample	Matric suction (kPa)	S (%)	Measured c_u (kPa)	Estimated c_u (kPa)	α from [66]	Back-calculated α
SAT-13%	0	100	11.5	11.5	0.9	0.71
ASCOMP-18%	55	83	58	60	0.82	0.7
ASCOMP-16%	110	65	68	71	0.67	0.57
ASCOMP-13%	205	44	80	62	0.75	0.79

consistent with the tests performed by Gan et al. [3] and Vanapalli et al. [5] on the same soil under drained conditions. A relatively faster loading rate of 1.4 mm/min was controlled to simulate undrained loading conditions.

The comparison between the measured from model tests and estimated shaft carrying capacity using the modified α , β and λ methods for UFG soil was shown in Fig. 16. The measured matric suction was 205 kPa, 110 kPa and 55 kPa for ASCOMP-13%, ASCOMP-16%, ASCOMP-18%, respectively. Table 2 shows the comparison between the measured and estimated undrained shear strength of IHT using Eq. (12). The determination of α values obtained from the correlation charts [66] and back-calculated from experimental results was also summarized in Table 2. The coefficient, $\beta = 0.3$ was used for both the saturated and unsaturated soils based on the value of soil–pile interface friction angle δ' . Vanapalli and Taylan [67] suggested a relationship between λ and the ratio of pile diameter to pile length d/L . A value of $\lambda = 0.32$ was used in the study. The results show significant increase in shaft carrying capacity due to the influence of matric suction. Also, the results calculated by the modified α , β and λ methods provide a good agreement with those measured results in model pile tests.

Summary

The bearing capacity and settlement behavior are two key properties required in the design of shallow and deep foundations. There is a strong relationship between the shear strength and the bearing capacity of soils. Due to this reason, geotechnical engineering pioneers have developed several approaches for determining the bearing capacity of shallow and deep foundations under drained and undrained loading conditions using the shear strength properties of the soils. These approaches are widely used in conventional engineering practice because they are simple and provide valuable information required for the design of foundations. However, the bearing capacity of foundations cannot be reliably determined by extending conventional soil mechanics principles for soils that are in a state of unsaturated condition. Significant research has been undertaken

during the past three decades for determining the shear strength of unsaturated soils. This paper summarizes the research that has been undertaken at the University of Ottawa, Canada during the past 15 years for determining, interpreting and predicting the bearing capacity of unsaturated soils in which shear strength of unsaturated soils has been used as a tool. The required information for extending these approaches includes the saturated shear strength parameters and the soil–water characteristic curve. The modified approaches for interpreting and predicting the bearing capacity of unsaturated soils are consistent with the approaches used for saturated soils in conventional geotechnical engineering practice. There is a good comparison between the predicted or estimated results from the proposed modified approaches and the experiments undertaken both in the laboratory and field for both shallow and deep foundations. The approaches proposed in this Companion Paper I are promising for implementing our present understanding of the mechanics of unsaturated soils into geotechnical engineering practice for determining the bearing capacity of unsaturated soils. More studies on different unsaturated soils that include large-scale field tests are necessary to better understand the strengths and limitations of the proposed modified approaches for use in the design of foundations in unsaturated soils. In future, foundation bearing capacity should also be determined in unsaturated soils to understand the influence of soil anisotropy. Additional studies that focus on the foundation under different loading conditions (e.g., dynamic loading) are necessary to improve the current understanding of the behavior of foundations in unsaturated soils.

Acknowledgement The authors would like to thank the Natural Science and Engineering Research Council of Canada for the research programs. Also, the authors appreciate the China Scholarship Council and University of Ottawa, Canada for the PhD research programs for Mengxi Tan and Xinting Cheng.

References

1. Fredlund DG, Morgenstern NR (1977) Stress state variables for unsaturated soils. *J Geotech Eng Div* 103(5):447–466
2. Fredlund DG, Morgenstern NR, Widger RA (1978) The shear strength of unsaturated soils. *Can Geotech J* 15:313–321

3. Gan JKM, Fredlund DG (1988) Multistage direct shear testing of unsaturated soils. American society for testing materials. *Geotech Test J* 11(2):132–138
4. Escario V, Sáez J (1986) The shear strength of partly saturated soils. *Géotechnique* 36(3):453–456
5. Vanapalli SK, Fredlund DG, Pufahl DE, Clifton AW (1996) Model for the prediction of shear strength with respect to soil suction. *Can Geotech J* 33(3):379–392
6. Nam S, Gutierrez M, Diplas P, Petrie J (2011) Determination of the shear strength of unsaturated soils using the multistage direct shear test. *Eng Geol* 122(3–4):272–280
7. Barbour SL (1998) The soil-water characteristic curve: a historical perspective. *Can Geotech J* 35(5):873–894
8. Zhai Q, Rahardjo H, Satyanaga A, Dai G (2019) Estimation of unsaturated shear strength from soil–water characteristic curve. *Acta Geotech* 14(6):1977–1990
9. Bishop AW (1959) The principle of effective stress. Lecture delivered in Oslo, Norway. *Technisk Ukeblad* 106(39):859–863
10. Terzaghi K (1943) *Theoretical soil mechanics*. Wiley, New York
11. Abramento, Carvalho (1989) Geotechnical parameters for the study of natural slope instabilization at Serra do Mar, Brazil. In: *Proceedings of 12th international conference on soil mechanics and foundation engineering*, Rio De Janeiro, Brazil, 13–18 August 1989, pp 1599–1602
12. Khalili N, Khabbaz MH (1998) A unique relationship for χ for the determination of the shear strength of unsaturated soils. *Géotechnique* 48(5):681–687
13. Shen D, Gens A, Fredlund DG, Sloan SW (2008) Unsaturated soils: from constitutive modelling to numerical algorithms. *Comput Geotech* 35:810–824
14. Fredlund DG, Xing A, Fredlund MD, Barbour SL (1996) Relationship of the unsaturated soil shear strength to the soil-water characteristic curve. *Can Geotech J* 33(3):440–448
15. Vanapalli SK, Fredlund DG (2000) Comparison of empirical procedures to predict the shear strength of unsaturated soils uses the soil-water characteristic curve. In: *Geo-Denver 2000*, American Society of Civil Engineers, Special Publication, vol 99, pp 195–209
16. Vanapalli SK (2009) Shear strength of unsaturated soils and its applications in geotechnical engineering practice. In: *Keynote address. Proceedings of 4th Asia-Pacific conference on unsaturated soils*. New Castle, Australia, November, pp 579–598
17. Oliveira OM, Marinho FAM (2003) Unsaturated shear strength behaviour of a compacted residual soil. In: *Proceedings of Asian conference on unsaturated soils: unsaturated soil geotechnical and geoenvironmental issues*. Osaka, Japan, pp 237–242
18. Garven EA, Vanapalli SK (2006) Evaluation of empirical procedures for predicting the shear strength of unsaturated soils. In: *Proceedings of 4th international conference on unsaturated soils, carefree, arizona*, American Society of Civil Engineers Geotechnical Special Publication, vol 147, no 2, pp 2570–2581
19. Mohamed FMO (2014) Bearing capacity and settlement behaviour of footings subjected to static and seismic loading conditions in unsaturated sandy soils. Doctoral dissertation, Université d'Ottawa/University of Ottawa
20. Donald IB (1957) Effective stresses in unsaturated non-cohesive soils with controlled negative pore pressure. M.Eng. Sc. thesis, University of Melbourne, Melbourne, Australia
21. Escario V, Juca J (1989) Shear strength and deformation of partly saturated soils. In: *Proceedings of 12th international conference on soil mechanics and foundation engineering*, Rio de Janeiro, vol 2, pp 43–46
22. Vanapalli SK, Mohamed FMO (2007) Bearing capacity of model footings in unsaturated soils. In: *Experimental unsaturated soil mechanics*. Springer, Berlin, pp 483–493
23. Kumbhojkar AS (1993) Numerical evaluation of Terzaghi's N_{γ} . *J Geotech Eng* 119(3):598–607
24. Vesic AB (1973) Analysis of ultimate loads of shallow foundations. *J Soil Mech Found Div* 99(SM1):45–73
25. Vanapalli SK, Oh WT (2010) Interpretation of the bearing capacity of unsaturated soils extending the effective and the total stress approaches, 6–8 September, Barcelona
26. Vanapalli SK, Oh WT (2010) Mechanics of unsaturated soils for the design of foundation structures. In: *Proceedings of the 3rd WSEAS international conference on engineering mechanics, structures, engineering geology*. World Scientific and Engineering Academy and Society (WSEAS), pp 363–377
27. Oh WT, Vanapalli SK (2011) Modelling the applied vertical stress and settlement relationship of shallow foundations in saturated and unsaturated sands. *Can Geotech J* 48(3):425–438
28. Oh WT, Vanapalli SK, Puppala AJ (2009) Semi-empirical model for the prediction of modulus of elasticity for unsaturated soils. *Can Geotech J* 46(8):903–914
29. Vanapalli SK, Oh WT (2010) A model for predicting the modulus of elasticity of unsaturated soils using the soil–water characteristic curve. *Int J Geotech Eng* 4(4):425–433
30. Oh WT, Vanapalli SK (2013) Interpretation of the bearing capacity of unsaturated fine-grained soil using the modified effective and the modified total stress approaches. *Int J Geomech* 13(6):769–778
31. Vanapalli SK, Oh WT, Puppala AJ (2007) Determination of the bearing capacity of unsaturated soils under undrained loading conditions. In: *Proceedings of the 60th Canadian geotechnical conference*. Can. Geotech. Soc., Alliston, pp 21–24
32. Skempton AW (1948) The $\phi_u=0$ analysis for stability and its theoretical basis. In: *Proceedings of the 2nd international conference of soil mechanics and foundation engineering*, vol 1, pp 72–77
33. Larson R (2001) *Investigations and load tests in clay till*, Sweden, Swedish Geotechnical Institute, Report 54
34. Rojas JC, Salinas LM, Seja C (2007) Plate-load tests on an unsaturated lean clay. In: *Schanz T (ed) Experimental unsaturated soil mechanics*. Springer, Berlin, pp 445–452
35. Oh WT, Vanapalli SK (2009) A simple method to estimate the bearing capacity of unsaturated fine-grained soils. In: *Proceedings of the 62nd Canadian geotechnical conference*, Halifax, Canada, pp 234–241
36. Chen JC (1984) Evaluation of strength parameters of partially saturated soils on the basis of initial suction and unconfined compression strength. M.Sc. thesis, Asian Institute of Technology Report, Bangkok, Thailand
37. Ridley AM (1993) The measurement of soil moisture suction. PhD thesis, University of London.
38. Babu GLS, Rao RS, Peter J (2005) Evaluation of shear strength functions based on soil water characteristic curves. *J Test Eval* 33(6):461–465
39. Pineda JA, Colmenares JE (2005) Influence of matrix suction on the shear strength of a compacted kaolinite under unconfined conditions: Shear strength prediction (Part 2). In: *Advanced experimental unsaturated soil mechanics*, pp 221–226
40. Vanapalli SK, Sheikhtaheri M, Oh WT (2018) Experimental and simple semi-empirical methods for interpreting the axial load versus settlement behaviors of single model piles in unsaturated sands. *Geotech Test J* 41(4)
41. Hansen JB (1970) A revised and extended formula for bearing capacity. *Danish Geotechnical Institute* 28, pp 5–11
42. Janbu N (1976) Static bearing capacity of friction piles. In: *Sechste Europaeische Konferenz Fuer Bodenmechanik Und Grundbau*, vol 1
43. Vanapalli SK, Taylan ZN (2012) Design of single piles using the mechanics of unsaturated soils. *Int J GEOMATE* 2(1):197–204

44. Skempton AW (1959) Cast in-situ bored piles in London clay. *Géotechnique* 9(4):153–173
45. Burland J (1973) Shaft friction of piles in clay—a simple fundamental approach. Publication of: *Ground Engineering/UK*, 6(3).
46. Vijayvergiya VN, Focht JA (1972) A new way to predict capacity of piles in clay. In: *Offshore technology conference*. Offshore Technology Conference
47. Costa YD, Cintra JC, Zornberg JC (2003) Influence of matric suction on the results of plate load tests performed on a lateritic soil deposit. *Geotech Test J* 26(2):219–226
48. Consoli NC, Schnaid F, Milititsky J (1998) Interpretation of plate load tests on residual soil site. *J Geotech Geoenviron Eng* 124(9):857–867
49. Mohamed FMO, Vanapalli SK (2006) Laboratory investigations for the measurement of the bearing capacity of an unsaturated coarse-grained soil. In: *Proceedings of 59th Canadian geotechnical conference*, Vancouver, BC, pp 1–4
50. Mohamed FMO, Vanapalli SK, Saatcioglu M (2011) Bearing capacity and settlement behavior of footings in an unsaturated sand. In: *The 14th Pan-American conference on soil mechanics and geotechnical engineering*, pp 1–8
51. Vanapalli SK, Mohamed FMO (2013) Bearing capacity and settlement of footings in unsaturated sands. *Int J Geomate* 5(1):595–604
52. Lins Y, Schanz T, Vanapalli SK (2009) Bearing capacity and settlement behavior of a strip footing on an unsaturated coarse-grained soil. In: *Proceedings of 4th Asia-Pacific conference on unsaturated soils*
53. Giddens R, Briaud J (1994) Load tests on five large spread footings on sand and evaluation of prediction methods. Texas, USA, Federal Highway Administration Department of Civil Engineering, Texas A&M University.
54. Mohamed FMO, Vanapalli SK (2015) Bearing capacity of shallow foundations in saturated and unsaturated sands from SPT–CPT correlations. *Int J Geotech Eng* 9(1):2–12
55. Mohamed FMO, Vanapalli SK, Saatcioglu M (2010) Comparison of bearing capacity of unsaturated sands using cone penetration tests (CPT) and plate load tests (PLT) in unsaturated soils: 1183–1188. CRS Press, Barcelona
56. ASTM D5778 (2007) Standard test method for electronic friction cone and piezocone penetration testing of soils. *Annual Book of ASTM Standards*, American Society of Testing Material, American Society of Testing Materials, West Conshohocken
57. Lee J, Salgado R (2005) Estimation of bearing capacity of circular footings on sands based on cone penetration test. *J Geotech Geoenviron Eng* 131(4):442–452
58. Adams MT, Collin JG (1997) Large model spread footing load tests on geosynthetic reinforced soil foundations. *J Geotech Geoenviron Eng* 123(1):66–72
59. Hanna A, Abdel-Rahman M (1998) Experimental investigation of shell foundations on dry sand. *Can Geotech J* 35(5):847–857
60. Dash SK, Sireesh S, Sitharam TG (2003) Model studies on circular footing supported on geocell reinforced sand underlain by soft clay. *Geotext Geomembr* 21(4):197–219
61. Bera AK, Ghosh A, Ghosh A (2007) Behaviour of model footing on pond ash. *Geotech Geol Eng* 25(3):315–325
62. ASTM D1586 (2011) Standard test method for standard penetration test (SPT) and split-barrel sampling of soils. *Annual Book of ASTM Standards*, American Society of Testing Material, American Society of Testing Materials, West Conshohocken.
63. Nabil (1985) Allowable pressure from loading tests on Kuwaiti soils. *Can Geotech J* 22(2):151–157
64. Al-Khazaali M, Vanapalli SK (2019) Experimental Investigation of single model pile and pile group behavior in saturated and unsaturated sand. *J Geotech Geoenviron Eng* 145(12):04019112
65. Power KC, Vanapalli SK (2010) Modified null pressure plate apparatus for measurement of matric suction. *Geotech Test J* 33(4):335–341
66. Sowers GB, Sowers GF (1951) Introductory soil mechanics and foundations. *Soil Sci* 72(5):405
67. Vanapalli SK, Taylan ZN (2011) Estimation of the shaft capacity of model piles in a compacted unsaturated soil. In: *Proceedings of 14th Pan-American conference on soil mechanics and geotechnical engineering & 64th Canadian geotechnical conference*
68. Han Z, Vanapalli SK, Kutlu ZN (2016) Modeling behavior of friction pile in compacted glacial till. *Int J Geomech* 16(6):D4016009

Publisher's Note Springer Nature remains neutral with regard to jurisdictional claims in published maps and institutional affiliations.